Stable Multidomain Structures Formed in the Process of Magnetization Reversal in GaMnAs Ferromagnetic Semiconductor Thin Films

D. Y. Shin, S. J. Chung, and Sanghoon Lee*
Physics Department, Korea University, Seoul 136-701, Korea

X. Liu and J. K. Furdyna
Physics Department, University of Notre Dame, Notre Dame, Indiana 46556, USA
(Received 22 June 2006; published 22 January 2007)

The process of magnetization reversal in ferromagnetic $Ga_{(1-x)}Mn_xAs$ epilayers has been systematically investigated using the planar Hall effect (PHE). Interestingly, we have observed a pronounced asymmetry in the PHE hysteresis when the range of the field scan is restricted to fields below the final magnetization transition. The observed behavior indicates that (a) multidomain structures are formed as $\boldsymbol{M}$ undergoes a reorientation, (b) the domain landscape formed in this way remains stable even after the magnetic field is switched off, and (c) the reorientation of magnetization directions corresponding to the transition points in PHE takes place separately within each domain.

DOI: 10.1103/PhysRevLett.98.047201 PACS numbers: 75.60.−d, 75.47.−m, 75.50.Pp, 75.70.−i

III-V-based ferromagnetic semiconductors such as $Ga_{(1-x)}Mn_xAs$ and $In_{(1-x)}Mn_xAs$ are considered to be highly promising in the field of spintronics because of their extraordinary spin properties that can be controlled by many external means [1–4]. Among the prominent features of these materials, magnetic anisotropy has recently received a great deal of attention due to the importance of this property in devices involving spin polarization [5–8]. Many experimental techniques [7–12] have been used to investigate this property in GaMnAs, providing a comprehensive picture of uniaxial and cubic crystalline anisotropy. The recently discovered giant planar Hall effect (PHE) [6] has enabled further detailed exploration of the process of magnetization switching between these magnetic easy axes in $Ga_{(1-x)}Mn_xAs$ films. Although intensive efforts have been made to understand the magnetization reversal process based on PHE [5,13] and magnetoresistance [6,14,15], only abrupt transitions between magnetic easy axes have so far been discussed, based on the single-domain model. In particular, the details of various mechanisms affecting the process of magnetization reorientation—especially those that tend to broaden this transition—have so far not been fully examined, either theoretically or experimentally.

Using extensive results of PHE measurements, in this Letter we report the observation of rather complicated domain behavior that occurs in the immediate region in which the magnetization $\boldsymbol{M}$ switches directions in $Ga_{(1-x)}Mn_xAs$ films. We will pay special attention to PHE hysteresis loops obtained by scans in which field turning points do not reach the second reorientation of $\boldsymbol{M}$ (which we will refer to as "minor loops"). As will be shown, the asymmetric behavior observed in such minor loops provides compelling evidence for the formation of multidomain structure in $Ga_{(1-x)}Mn_xAs$ layers during the process of magnetization reversal. Although in this Letter we focus on results obtained on a single representative $Ga_{(1-x)}Mn_xAs$ sample, the observed asymmetry in PHE is a general feature that we have observed in many other $Ga_{(1-x)}Mn_xAs$ films with different Mn concentrations and specimen sizes.

The representative sample is in the shape of a 400 μm wide and 2500 μm long rectangle Hall bar device, with the long dimension along the [110] direction, fabricated from molecular beam epitaxy grown 100 nm $Ga_{(1-x)}Mn_xAs$ film, with $x \approx 0.038$, as shown in Fig. 1(a). The detail experimental process will be given elsewhere. The PHE measured at $\varphi = 200°$ is shown in Fig. 1(c), in which the field was swept between −250 and +250 G. The two-step switching behavior in planar Hall resistance R_{xy} is similar to that observed by other investigators in $Ga_{(1-x)}Mn_xAs$ epilayers [5,13,16,17] and, as a first approximation, can be understood in terms of the magnetic energy of a single in-plane magnetic domain, given by [5]

$$E = -K_c \cos^2(2\varphi)/4 + K_u \sin^2\varphi - MH\cos(\theta - \varphi), \quad (1)$$

where K_c and K_u are the cubic and uniaxial magnetocrystalline anisotropy constants, respectively, H is the external magnetic field, M is the magnetization, and φ and θ are the angles of H and M relative to the [110] direction, respectively. It is now well established that at low temperatures the cubic anisotropy is normally stronger in $Ga_{(1-x)}Mn_xAs$ than the uniaxial anisotropy (i.e., $K_c > K_u$), although the effect can be reversed with increasing temperature and/or carrier concentration [18,19]. Since in this investigation the measurements were performed at 2.8 K, we will therefore as a first approximation ignore the effect of uniaxial anisotropy. The plot of magnetic energy in the absence of H in Fig. 1(b) clearly shows four stable states of $\boldsymbol{M}$ along the [100], [010], [$\bar{1}$00], and

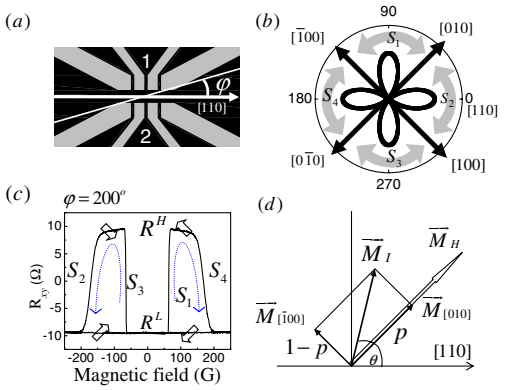

FIG. 1 (color online). (a) Schematic diagram for Hall device structures and directions for current flow and magnetic field. The Hall voltage is measured between the two leads marked as 1 and 2 in the Hall diagram. (b) Polar plot of magnetic energy and the corresponding easy axes. (c) Planar Hall resistance taken at $\varphi = 200°$ as a function of the in-plane magnetic field. The thick arrows on each plateau indicate the direction of magnetization in single-domain states. (d) Configuration of two orthogonal magnetic domains for an intermediate states R^{I1} producing a resultant magnetization $\vec{M}_I$ between two easy axes. Here $\vec{M}_H$ shows magnetization along the [010] direction when the entire sample is in a single-domain state.

$[0\bar{1}0]$ crystallographic directions, i.e., the four in-plane magnetic easy axes determined by cubic anisotropy. This simple model provides a good description of the double hysteresis in Fig. 1(c) in terms of a two-step switching process of $\boldsymbol{M}$ between these easy axes.

For a ferromagnetic system with in-plane magnetic anisotropy, the in-plane field H leads to a planar Hall resistance R_{xy}, given by the well-known expression [20]

$$R_{xy} = \frac{k}{t} M^2 \sin 2\theta, \tag{2}$$

where M is the magnetization, t is the film thickness, and θ is the angle between the directions of I and M, as shown in Fig. 1(d). The constant k is related to the anisotropic magnetoresistance (i.e., the difference between the resistivities for $\boldsymbol{M}$ parallel and perpendicular to the current direction). The directions of $\boldsymbol{M}$ at each successive plateau in the PHE spectrum occurring during the up-and-down field sweeps are indicated by arrows in Fig. 1(c) and correspond to the [010], $[\bar{1}00]$, $[0\bar{1}0]$, or [100] easy axes. To facilitate discussion, in what follows we will refer to the states corresponding to the maximum and minimum values of R_{xy} as R^H and R^L, respectively, and we will designate the switching process $[010] \leftrightarrow [\bar{1}00]$ as S_1, $[100] \leftrightarrow [010]$ as S_2, $[0\bar{1}0] \leftrightarrow [100]$ as S_3, and $[\bar{1}00] \leftrightarrow [0\bar{1}0]$ as S_4, as indicated in Fig. 1(b). The direction of $\boldsymbol{M}$ in the spectra shown in Fig. 1(c) is seen to undergo a 360° ''round-trip'' via the switching sequence S_3, S_2, S_1, and S_4.

Careful inspection of the PHE spectra reveals that the transition at the switching field is not an abrupt process, especially for the second switching, i.e., that occurring at the higher field for each sweep direction [marked as S_2 and S_4 in Fig. 1(c)]. Such nonabrupt transitions have been observed in GaMnAs by many other investigators [5,13,16,17], but their interpretation was usually approximated by abrupt switchings of magnetization, consistent with the single-domain model. However, the appearance of such nonabruptness in the transition of $\boldsymbol{M}$ is quite important, since it suggests a more complex process of magnetization reversal, involving a multidomain reorientation. Specifically, the existence of an intermediate value of R_{xy} in the nonabrupt transition region indicates that the direction of $\boldsymbol{M}$ at that moment lies between the two axes corresponding to R^H and R^L. This intermediate direction of $\boldsymbol{M}$ in the film can be realized either by a coherent rotation of a single magnetic domain toward the direction of the applied field $\boldsymbol{H}$ or by the magnetization of a multidomain system, with the local $\boldsymbol{M}$ in each domain oriented along one of the two orthogonal easy axes.

To identify the correct domain structure (single or multidomain) of the film at the moment of transition (i.e., at the intermediate value of R_{xy} between R_H and R_L), we have taken PHE data using minor loop scans (i.e., loops in which the field turning points stop just short of the complete upper-field rotation of $\boldsymbol{M}$), as follows. After we saturate the magnetization in one direction, we reduce the field, cross the zero, stop at some chosen value H_i within the hysteresis region (which becomes the turning point of the scan), and then reverse the sweep direction to complete the round-trip scan between H_i and $-H_i$. The minor PHE hysteresis loops obtained for different turning points H_i are shown in Fig. 2. The specific turning points used to obtain the minor loops in Figs. 2(b), 2(c), and 2(e) are marked by arrows on the main (full) hysteresis loop in Fig. 2(a). In the minor loop in Fig. 2(b), R_{xy} is reversible in the part of the field region between $+H_b$ and $-H_b$ (the turning points $\pm H_b$ being just beyond the first switching field) and exhibits a nearly square single hysteresis behavior between the two states R^H and R^L, indicating a single-domain state in the entire sample, as is usually assumed in analyzing the reversal process of $\boldsymbol{M}$. It is, however, interesting to note that in Figs. 2(c) and 2(e) the value of R_{xy} is not reversible when the magnetic field loop is swept out between $\pm H_c$ or $\pm H_e$ [i.e., between points (c) and (e) marked by arrows in Fig. 2(a) on the broad slope at the second reorientation of $\boldsymbol{M}$]. Using Fig. 2(c) as an example, we note that on the return path the value of R_{xy} remains the same as it was at the turning field H_c (marked as R^{I1}), all the way until the first transition after the field is reversed. This is quite surprising, since—if the transition involves a coherent single-domain rotation—on the return trip one would expect the value of R_{xy} to trace out exactly the same path as it did in the incoming path. The constant value of R_{xy} (marked as state R^{I1}) indicates therefore that the multidomain structure formed at the point marked (c) during the second switching process remains essentially ''frozen'' as the magnetic field is reduced, all the way past $H = 0$, until one reaches the first switching field in the reverse direction,

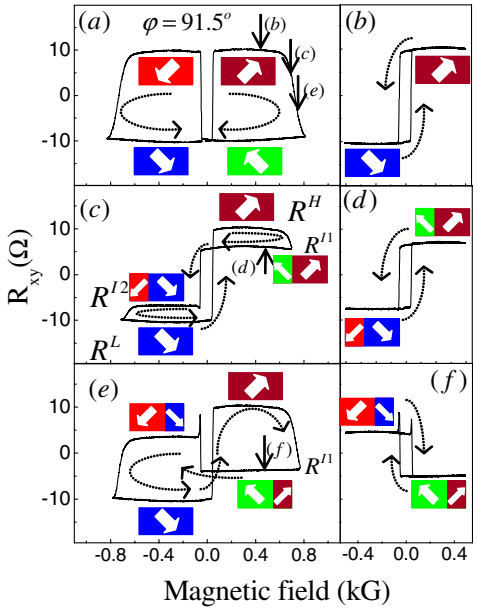

FIG. 2 (color online). (a) Full hysteresis loop of planar Hall resistance R_{xy} measured at $\varphi = 91.5°$. Minor hysteresis loops obtained at different field scan ranges are shown in (b), (c), and (e), with corresponding turning fields indicated by arrows in (a). Note the asymmetry of the loops in (c) and (e). The subfield loops corresponding to (c) and (e), with respective turning fields indicated by arrows, are shown in (d) and (f). The direction of the field sweep is indicated by dotted arrows in each panel.

as seen in the loop in Fig. 2(c). Recently, magnetization imaging experiments performed on a $Ga_{(1-x)}Mn_xAs$ layer have clearly demonstrated the nucleation and rapid propagation of magnetic domains during the reorientation of $\boldsymbol{M}$ [18,21].

The first switching on the negative field side in Fig. 2(c) is even more surprising, since upon reaching that field the value of R_{xy} do not jump to the R^L state but to an intermediate value of R_{xy} marked as state R^{I2}, which remains constant as H increases in the negative direction almost (but not all the way) to the turning field $-H_c$. As the field approaches the negative turning point $-H_c$, the value of R_{xy} finally drops from its stable intermediate state R^{I2} to R^L, as seen on the left in Fig. 2(c). Since the value of R_{xy} is determined by the angle between the magnetization and the current, the intermediate value of the state R^{I2} implies that the $\boldsymbol{M}$ of the sample lies between the two easy axes defined in Fig. 1(b) (i.e., between the $[0\bar{1}0]$ and [100] directions). Such stable intermediate orientation of $\boldsymbol{M}$ can be achieved only by a vector sum of mutually orthogonal magnetic domains with $\boldsymbol{M}$ along the two easy axes.

The fractions of the sample area corresponding to the orthogonal magnetic domains at the moment of transition can be determined from the value of R_{xy} by finding the corresponding average direction of $\boldsymbol{M}$ based on Eq. (2) and the magnetization configurations shown in Fig. 1(d). From Fig. 1(d), one can find the relations $M_{[010]} = p|M_H|$, $M_{[\bar{1}00]} = (1-p)|M_H|$, $M_I = \sqrt{p^2 + (1-p)^2}|M_H|$, and $\varphi = \tan^{-1}(\frac{1-p}{p}) + \frac{\pi}{4}$, where p is the fraction of the area corresponding to domains that are defined in the state R^H (i.e., with $\boldsymbol{M}$ along [010] or $[0\bar{1}0]$), and the fraction of the area with domains in the R^L state (i.e., along [100] or $[\bar{1}00]$) is given by $1-p$. The PHE values for R^H and R^I are obtained by inserting the above relations into Eq. (2), and simple algebra leads to an expression for p corresponding to a given R^I as $p = (R^I + R^H)/(2R^H)$.

In the data shown in Fig. 2(c), the R_{xy} value of R^{I1} then indicates that $p = 0.8$ (80% of the domains correspond to magnetization along [010] and 20% to $\boldsymbol{M}$ along $[\bar{1}00]$), while the R_{xy} value in state R^{I2} gives $p = 0.2$ (indicating that the system consists of 80% of [100] domains and 20% of $[0\bar{1}0]$ domains). This suggests that the magnetization switching occurs independently in these two fractions of the sample area: In the transition from R^{I1} to R^{I2} states, 80% of the area switches $\boldsymbol{M}$ from $[010] \rightarrow [100]$ and 20% of the area from $[\bar{1}00] \rightarrow [0\bar{1}0]$. That is, domains with the two orthogonal magnetizations (i.e., along [010] and $[\bar{1}00]$) formed in the switching process each rotate by 90° in the opposite sense (i.e., one clockwise, the other counterclockwise) independently within each domain, while the domain walls remain intact, as schematically shown in Fig. 2.

Such interesting asymmetric loops can be obtained in different field ranges as long as the maximum magnetic fields (i.e., the turning points of the field sweep) are in the region of the second transition, as shown in Fig. 2(e). Note that the fraction of magnetic domains with $\boldsymbol{M}$ along $[\bar{1}00]$ (corresponding to the state R^L) in the right-hand loop in Fig. 2(e) is increased relative to what it was in Fig. 2(c), and the same larger fraction jumps to the $[0\bar{1}0]$ orientation (larger R^H component) in the left loop in Fig. 2(e), i.e., after the first switching in the negative field direction.

The assumption of stable domain walls and of independent reorientation of $\boldsymbol{M}$ within each domain is further supported by taking still shorter field scans than those used to sweep out Figs. 2(c) and 2(e), as follows. After reaching the turning field in the minor loops in Figs. 2(c) and 2(e), the field is reduced to a lower value [marked by arrows (d) and (f) in Figs. 2(c) and 2(e), respectively], and PHE is measured in the corresponding round-trip scans $\pm H_d$ and $\pm H_f$. Such subfield loops for Figs. 2(c) and 2(e) are shown on the right-hand side in Fig. 2, showing a nearly square single hysteresis behavior between the two states R^{I1} and R^{I2}. This phenomenon indicates that the multidomain structures comprising states R^{I1} and R^{I2} are stable and that 90° magnetization switching events [$[010] \leftrightarrow [100]$ and $[\bar{1}00] \leftrightarrow [0\bar{1}0]$, corresponding to S_2 and S_4 transitions in Fig. 1(b)] occur within individual domains in these subfield scans.

Magnetization switching in a multidomain structure generates another distinct feature in the magnetization reversal process. Notice the appearance of sharp spikes at the first switching field in the minor loops and in the corresponding subfield loops in Fig. 2 [this effect is prominent in Figs. 2(e) and 2(f)]. Interestingly, these first-switch-

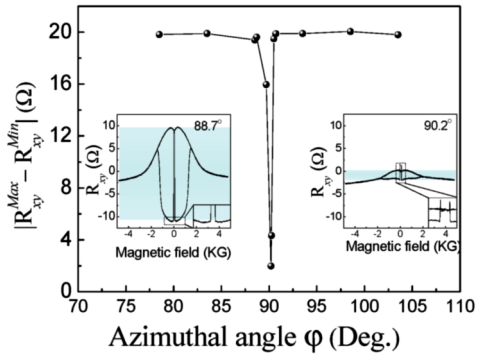

FIG. 3 (color online). Angular dependence of the largest value of $|R_{xy}^{\max} - R_{xy}^{\min}|$ observed in the planar Hall resistance. The value exhibits a sharp dip near the angle $\varphi = 90°$, i.e., when the applied field is nearly aligned with the $[\bar{1}10]$ hard axis of $\boldsymbol{M}$. The examples of planar Hall resistance spectra taken at two different orientations of $\boldsymbol{H}$ near the $[\bar{1}10]$ hard axis are shown in the insets. The maximum amplitude $|R_{xy}^{\max} - R_{xy}^{\min}|$ of each loop (i.e., the width of the shaded region) is very sensitive to the field direction. The sharp peaks appearing at the first switching field are characteristic of magnetization switching in multidomain structures. This feature is magnified in the insets.

ing-field spikes are absent in sweeps in the positive field direction, where the magnetization switching occurs between single-domain states (i.e., from R^L to R^H states). Since the single-domain states correspond to either a maximum or a minimum value of R_{xy}, the transition from one state to the other (i.e., either $[100] \leftrightarrow [010]$ or $[\bar{1}00] \leftrightarrow [0\bar{1}0]$) will lead to an abrupt jump between the two extreme values at a single switching field. The situation, however, is different when the transition occurs between multidomain states (i.e., for transition from R^{I1} to R^{I2} states). In this case, domains with $\boldsymbol{M}$ along the [010] and $[\bar{1}00]$ directions experience $[010] \leftrightarrow [100]$ and $[\bar{1}00] \leftrightarrow [0\bar{1}0]$ transitions, respectively. The switching field for these two transitions can be slightly different, since the angle between the directions of $\boldsymbol{H}$ and of $\boldsymbol{M}$ is different for the [010] and the $[\bar{1}00]$ domains. This slight difference in the switching field for the two domain families allows a narrow magnetic field window where the magnetization in all domains in the sample is collinear with either the R^L or the R^H state (although directions of $\boldsymbol{M}$ in the two domain families are antiparallel). This transient configuration of the magnetic domains produces sharp spikelike peaks (or dips) at the switching field in the minor loops seen in Fig. 2.

The formation of multidomain structures in the magnetization reversal process is extremely sensitive to the direction of the applied magnetic field. In Fig. 3, we plot the largest amplitude of R_{xy} (i.e., the width of the shaded region in the inset in Fig. 3, $|R_{xy}^{\max} - R_{xy}^{\min}|$) as a function of the azimuthal angle φ. The value of $|R_{xy}^{\max} - R_{xy}^{\min}|$ remains constant up to a few degrees from the $[\bar{1}10]$ hard axis and shows a sudden dramatic decrease near $\varphi = 90°$ (i.e., close to the $[\bar{1}10]$ hard axis). Since the maximum value of 20Ω for $|R_{xy}^{\max} - R_{xy}^{\min}|$ (i.e., the difference between states R^H and R^L) can be attained only via a 90° rotation of the total magnetization $\boldsymbol{M}$ between the two easy axes, the magnetization of the sample is in a single-domain state during the reversal process when the magnetic field direction is several degrees away from the hard axis. The values of $|R_{xy}^{\max} - R_{xy}^{\min}|$ smaller than 20Ω appearing in the very narrow region of φ near 90° (i.e., near $\boldsymbol{H}$ parallel to $[\bar{1}10]$) indicate that in that narrow window the direction of the total (i.e., resultant) $\boldsymbol{M}$ does not lie along one of the two easy axes but somewhere in between. As argued earlier, however, this situation can be understood as a combination of magnetizations in different domains, with $\boldsymbol{M}$ in each domain oriented along one of two orthogonal easy axes. This can be further supported by the appearance of the sharp spikes at the first switching field only in PHE spectra, in which the value of $|R_{xy}^{\max} - R_{xy}^{\min}|$ is smaller than 20Ω. An example is given in right side inset in Fig. 3, as shown in the zoomed-in insets.

In conclusion, we have observed interesting phenomena arising from the multidomain structure in PHE at magnetization switching fields. The striking asymmetry of the minor PHE hysteresis loops suggests that—once the multidomain structure is formed—the magnetization switching occurs individually within each domain, while the domain walls remain unchanged. The robust stability of the multidomain structure described in this study thus provides an interesting opportunity for multistate memory devices, with ample opportunities for manipulation.

This research was supported by NSF Grant No. DMR06-03752, by Korea Research Foundation Grant No. KRF-2004-005-C00068, by KOSEF through the QSRC at Dongguk University, and by the Seoul R&BD Program.

*Electronic address: slee3@korea.ac.kr

[1] H. Ohno *et al.*, Nature (London) **408**, 944 (2000).
[2] A. Twardowski, Acta Phys. Pol. A **98**, 203 (2000).
[3] S. Koshihara *et al.*, Phys. Rev. Lett. **78**, 4617 (1997).
[4] S. Lee *et al.*, J. Appl. Phys. **93**, 8307 (2003).
[5] H. X. Tang *et al.*, Phys. Rev. Lett. **90**, 107201 (2003).
[6] H. X. Tang and M. L. Roukes, Phys. Rev. B **70**, 205213 (2004).
[7] G. P. Moore *et al.*, J. Appl. Phys. **94**, 4530 (2003).
[8] X. Liu *et al.*, Phys. Rev. B **67**, 205204 (2003).
[9] X. Liu *et al.*, Phys. Rev. B **71**, 035307 (2005).
[10] M. Sawicki, J. Magn. Magn. Mater. **300**, 1 (2006).
[11] M. Sawicki *et al.*, Phys. Rev. B **70**, 245325 (2004).
[12] D. V. Baxter *et al.*, Phys. Rev. B **65**, 212407 (2002).
[13] A. W. Holleitner *et al.*, Appl. Phys. Lett. **85**, 5622 (2004).
[14] K. Hamaya *et al.*, IEEE Trans. Magn. **39**, 2785 (2003).
[15] K. Hamaya *et al.*, IEEE Trans. Magn. **40**, 2682 (2004).
[16] K. Y. Wang *et al.*, Phys. Rev. B **72**, 085201 (2005).
[17] H. X. Tang *et al.*, Nature (London) **431**, 52 (2004).
[18] U. Welp *et al.*, Phys. Rev. Lett. **90**, 167206 (2003).
[19] L. V. Titova *et al.*, Phys. Rev. B **72**, 165205 (2005).
[20] K. Okamoto, J. Magn. Magn. Mater. **35**, 353 (1983).
[21] M. Yamanouchi *et al.*, Phys. Rev. Lett. **96**, 096601 (2006).